ELSEVIER

Physica B 248 (1998) 217–222

PHYSICA B

Liquid-like interfacial correlation in LB films

M.K. Sanyal*, J.K. Basu, A. Datta

Surface Physics Division, Saha Institute of Nuclear Physics, 1/AF, Bidhannagar, Calcutta 700 064, India

---

Abstract

We present here results of X-ray reflectivity and diffuse scattering study of three Langmuir–Blodgett films, all having nine monolayers. These systems are the cadmium arachidate film grown using the conventional method, the arachidic acid film with trapped CdS layers at the interfaces formed by exposing the cadmium arachidate film to hydrogen sulphide and ferric stearate film grown from a monolayer of the pre-formed salt on water. Self-consistent analysis of all the scattering data measured, viz., in specular, in transverse and in longitudinal directions, for each film shows that the interfaces are conformal in nature and the logarithmic in-plane correlation, characteristic of capillary waves on liquid surfaces, exists in all the three films. © 1998 Elsevier Science B.V. All rights reserved.

PACS: 68.18. + p; 61.46. + w; 68.10. − m; 68.55. − a

Keywords: Langmuir–Blodgett films; X-ray reflectivity; Diffuse scattering

---

1. Introduction

Systematic analysis of specular reflectivity data provides us the electron density profile, and in turn compositional profile as a function of depth [1]. Diffuse scattering studies, on the other hand, gives us information regarding correlation of various interfaces present in the system under study [2]. In most cases, one can separate out [3,4] specular and off-specular components of scattering and analyse them separately. But for systems having large in-plane correlation length, it becomes impossible to separate out these components [2] because the diffuse intensity peaks near the specular ridge. In these cases analysis of measured data is done by calculating total scattering profiles in various directions in reciprocal space (q_x, q_y and q_z) [3,5].

Langmuir–Blodgett (LB) films are deposited by a simple process, that involves the sequential transfer of an organic monolayer, spread normally on water, by repeated dipping of a substrate [6,7]. The quality of interfaces are generally excellent and one can measure X-ray reflectivity up to a very large scattering angle. LB films of fatty acid salts are generally formed by spreading a corresponding fatty acid monolayer on water containing dissolved inorganic salt. In this method the number of metal ions and the number of acid molecules available are not equal. This introduces a large uncertainty in the composition of the

---

* Corresponding author. Tel.: + 91 37 534549; fax: + 91 33 374637; e-mail: milan@cmp.saha.ernet.in.

PII: S0921-4526(98)00235-X

monolayer, and, in general, the actual mechanism of salt formation during the transfer of the monolayer to the substrate is not clear so far. However, if an LB film is deposited from a monolayer of a preformed salt of a fatty acid, such as ferric stearate (FeSt) on water, at least the uncertainty in the monolayer composition is much reduced.

Our understanding regarding the nature of correlation in the interfaces [8] and the nature of molecular stack [9] in these films are also far from complete. The stability of the interfaces present in these films are intriguing, too. It was shown recently that by exposing a cadmium arachidate (CdA) LB film in an hydrogen sulphide (H_2S) environment, cadmium sulphide (CdS) nanostructures can be formed [10] without much disturbance to the embedding LB structure. We have performed an X-ray scattering study of three LB films to understand the nature of interfaces present in these systems and to probe molecular arrangements in these films. In the next section we have described these films and in the third section we have outlined the experimental details and the formalism used to analyse the measured X-ray scattering data. In the last section the main results are discussed.

2. The LB films

Two LB films of cadmium arachidate (CdA), each 9 monolayer (ML), were deposited on quartz substrates from a spread monolayer of arachidic acid (AA) on an aqueous solution of cadmium chloride (4×10^{-4} M) at a surface pressure, temperature and pH of 30 mN m^{-1} (surface tension 42 mN m^{-1}), 10°C and 6.4, respectively. The deposition rate was 10 mm/min. Of these films one was exposed to H_2S gas for 60 mins. The details of the experimental arrangement used to prepare these LB films has been described earlier [11]. In the UV–VIS absorbance data taken on these films the absorption edge for the H_2S exposed film was found to be at 455 ± 5 nm indicating the formation of nanocrystalline CdS in this film [10,11].

Ferric stearate (FeSt) was prepared by adding a measured amount of ferric sulphate solution to freshly prepared sodium stearate solution in hot, distilled water until the residual solution was slightly alkaline (pH $\simeq$ 8.0). Fourier transform infra red spectra of the purified bulk FeSt sample, as well as a 11 ML LB film of this FeSt on calcium fluoride, could not detect the presence of hydroxy fatty acid salts. A 9 ML LB film of this preformed and purified FeSt was deposited on a Si(1 0 0) substrate at a surface pressure, temperature and subphase (water) pH of 30 mN m^{-1} (surface tension 42 mN m^{-1}), 25°C and 5.6, respectively. The deposition rate was 3 mm/min. Details of the sample preparation, purification and LB deposition have been provided elsewhere [12].

3. X-ray scattering study

X-ray specular reflectivity measurements were performed on these films by keeping the angle of incidence (α) equal to the angle of reflection (β) while the diffuse scattering data were taken by keeping these angles unequal [3,5]. The data was collected using a triple axis spectrometer (optix microcontrole) with Cu $K_{\alpha 1}$ X-rays obtained from a rotating anode generator (FR 591, Enraf Nonius) and a Si(1 1 1) monochromator. The incident beam was collimated by slits having horizontal and vertical apertures of 100 and 5000 μm, respectively, with the horizontal aperture determining the width of the incident beam in the scattering plane. In case of diffuse scattering measurements the scattered beam was defined in the scattering plane by a horizontal slit of aperture 100 μm, placed in front of the detector. The vertical aperture of the detector slit was kept wide open to effectively integrate [3,5] the out-of-plane component of the scattering.

The specular reflectivity data indicate that the intensity of the multilayer Bragg peaks in all the films increase with increasing horizontal detector slit width even beyond the beam divergence width. Moreover in a log–log plot the scattered intensity was found to decay linearly, with a slope $(\eta - 1)$, as a function of the in-plane scattering vector q_x, where η depends on q_z. These results clearly indicate that we are dealing with scattering which has a strong diffuse component around the specular ridge similar to that observed in scattering from liquid surfaces [5,13] with logarithmic height–height correlation due to the presence of capillary waves. It is also evident that the longitudinal off-specular scans follow the specular profiles quite closely. So the multiple interfaces present in the system are highly conformal [3,4]. It is known that beyond a certain critical in-plane length, r_c, interfaces in organic multilayer films behave as a correlated system [14,15], exhibiting a single logarithmic height–height correlation for all the interfaces. The value of r_c depends on the compressibility of the film and decreases with decreasing compressibility [14]. Hence in analogy with these theoretical formulations and using our earlier expression [5] for liquid surfaces, we can write down $g(r)$ for the interfaces present in our LB films as

$$g_{ij}(r) = \sigma_i^2 + \sigma_j^2 + B\gamma_E + B\ln(\kappa r/2), \qquad (1)$$

where σ_i, σ_j are the rms roughnesses of the ith and jth interfaces, B is given by $\kappa_B T/\pi\gamma$, and κ is the low wave vector cutoff for capillary waves in LB films decided by van der Waals interactions and can be written as [16,17] $\kappa^2 = A/2\pi\gamma d^4$, where A is the effective Hamaker constant, γ is the interfacial tension and d is the total film thickness.

In our experiments, as mentioned earlier, we have kept the out-of-plane wave vector resolution (Δq_y) coarse so that the q_y integration in the structure factor is effectively performed during data collection [3,5]. Using a gaussian resolution function for q_x, obtained from the direct beam profile, we can write the expression [5] for the detected scattered intensity, $I(q_x,q_z)$, in terms of the Kummer function and gamma function as

$$\begin{aligned} I(q_x, q_z) &= I_0 \frac{R(q_z)q_z}{2k_0 \sin\alpha} \\ &= \frac{1}{\sqrt{\pi}}\Gamma\left(\frac{1-\eta}{2}\right) {}_1F_1\left(\frac{1-\eta}{2};\frac{1}{2};\frac{-q_x^2L^2}{4\pi^2}\right), \end{aligned} \qquad (2)$$

where $R(q_z)$ is the specular reflectivity as a function of q_z for a multilayer and the other terms are as explained in Ref. [5].

In the specular condition ($q_x = 0$), the Kummer function becomes unity and $2k_0 \sin\alpha$ cancels with q_z; Eq. (2) gives us the effective reflectivity as obtained earlier [5] for liquid–vapour interfaces. The reflectivity profile, $R(q_z)$ was calculated using a slicing technique [18,19] with the effective roughness, $(\sigma_{\mathrm{eff}})_i$ given by

$$(\sigma_{\mathrm{eff}})_i^2 = \sigma_i^2 + \tfrac{1}{2}B\gamma_E - \tfrac{1}{2}B\ln(2\pi/\kappa L). \qquad (3)$$

Here the actual roughness of an interface, σ_i, is more than the measured effective roughness, $(\sigma_{\mathrm{eff}})_i$.

4. Results and discussions

The results of the analysis of a CdA film is presented in Fig. 1. In the lower panel the specular reflectivity data ($q_x = 0$) along with the fit (solid line) is shown as (a). It was observed that a simplified model (shown in the inset) can mimic the main features of the reflectivity data. In this simplified model the number of slices used to represent the

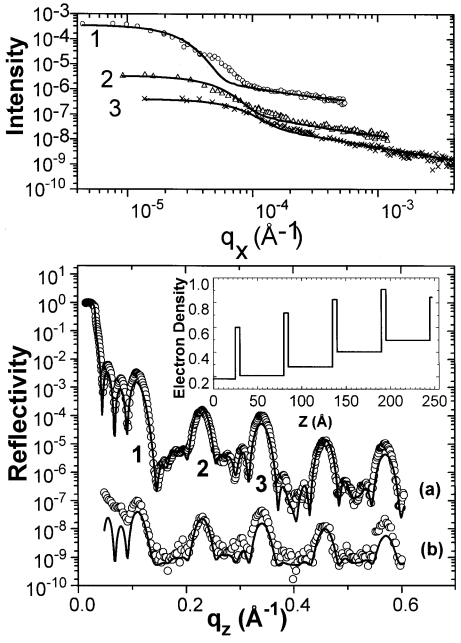

Fig. 1. Lower panel: (a) specular reflectivity, (b) off-specular longitudinal and obtained electron density (electrons/Å^3) profiles (in inset) for the unexposed cadmium arachidate LB film (9 monolayers) are shown. The solid line in (a) and (b) are calculated profiles obtained from the model shown in inset. Upper panel: transverse diffuse scattering data measured at the first three Bragg peak positions (1, 2 and 3 in the lower panel) shown along with the fitted curves (solid lines). Refer to the text for details.

electron density profile (EDP) is minimized. Although one can get a perfect fit to the reflectivity data by increasing the number of slices to represent the details of the EDP, the essential features of the EDP remains unchanged [20]. The obtained EDP (shown in the inset of Fig. 1) indicates the increase in the absolute values of electron densities in each bilayer as a function of depth, possibly resulting from an increased disorder and formation of patches due to incomplete film coverage, towards the top of the film ($z = 0$). This feature is common to all the three LB films presented.

In the EDP the Cd positions are indicated by the higher electron density boxes. The total film thickness was found to be 247.5 Å which is equal to 4.5 times the obtained bilayer spacing of 55 Å, as expected for the 9 ML film. The fitted values obtained for σ_{eff} were 2.1 ± 0.1 Å for the air-film interface and 2.0 ± 0.2 Å for all the other interfaces.

The upper panel of Fig. 1 shows three sets of transverse scans taken at the 1st, 2nd and 3rd Bragg peaks, at q_z values of 0.108, 0.228, 0.34 Å^{-1}, respectively. All the curves were fitted using Eq. (2) (solid line). Only B and the additive constant background, arising mainly due to dark counts, were allowed to vary in order to obtain a consistent fit of all these data. The value of B obtained from this analysis was 2.1 ± 0.2 Å^2 giving an effective surface tension of 62.8 mN m^{-1} (at 27°C).

Along with the specular data, we have shown the longitudinal diffuse data taken with a constant angular offset of 1.0 mrad (as (b) in the lower panel). The parameters obtained from fitting the transverse diffuse and specular data, namely B, $(\sigma_{\mathrm{eff}})_i$ and background counts, were used to calculate longitudinal diffuse scattering profiles (solid line) to check self-consistency of the analysis scheme. The excellent agreement of the calculated profile with the measured data demonstrates the assumed conformality of the interfaces.

For the exposed CdA film the specular reflectivity data and fit (solid line) is shown in the lower panel of Fig. 2 and the obtained EDP is shown in the inset. We have used 36 slices, each having a thickness of 7 Å, to represent the EDP. The total film thickness and the bilayer spacing was found to be 252 Å and is 56 Å respectively. The obtained values for σ_{eff} for this film were 2.1 ± 0.1 Å for the air–film interface and 2.0 ± 0.2 Å for the other interfaces. We should mention here that calculations based on a simple model for the EDP with slices of size 14 Å, which is a quarter of the bilayer thickness, around the metal sites in the film correctly brings out the most prominent feature in the measured reflectivity profile, i.e. vanishing of the fourth Bragg peak. However, the quality of the overall fit to the data is significantly improved by using the detailed model (shown in the inset). The observed rounding of EDP around metal sites in the obtained model of the film is mainly due to variation of size and orientation of CdS nanoparticles (as projected in the z direction) and due to the presence of capillary waves at the interfaces. These details will be presented elsewhere [20].

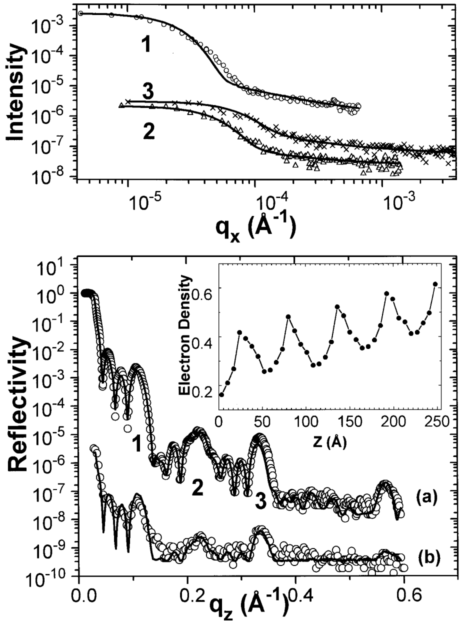

Fig. 2. Lower panel: (a) specular reflectivity, (b) off-specular longitudinal and obtained electron density (electrons/Å^3) profiles (in inset) for cadmium archidate LB film (9 monolayers) exposed to hydrogen sulphide (60 min) are shown. The solid line in (a) and (b) are calculated profiles obtained from the model shown in inset. Upper panel: transverse diffuse scattering data measured at the first three Bragg peak positions (1, 2 and 3 in the lower panel) shown along with the fitted curves (solid lines). Refer to the text for details.

The upper panel of Fig. 2 shows three set of transverse scans measured at the 1st, 2nd and 3rd

Bragg peaks, at q_z values of 0.107, 0.22, 0.33 Å^{-1}, respectively. The data were fitted (solid lines) in a manner similar to that for the unexposed film and the obtained value for B was 2.1 ± 0.2 Å^2 same as for the former.

Along with the specular data (a), we have shown the longitudinal diffuse data (b) taken with a constant angular offset of 0.8 mrad. Self-consistent analysis to the data was performed as in the earlier case and the fit is shown (solid line) as (b) in Fig. 2. The agreement of the calculated profile with the measured data demonstrates the assumed conformality of the interfaces inspite of the formation of CdS at the interfaces.

The lower panel of Fig. 3 shows the specular data for the FeSt LB film. The solid line is the reflectivity profile calculated from the EDP shown in the inset. We have used 45 slices of 5 Å thickness to represent this EDP. In the upper panel of this figure we have shown the asymptotic tails of the transverse diffuse scattering data taken at the 1st, 2nd 3rd Bragg peaks, at q_z values of 0.118, 0.249, 0.375 Å^{-1}, respectively. Unlike the other two films, we could not analyse the transverse data upto the central region due to a split observed in the specular peak. We feel that this split is due to misoriented domains in the film. It should be noted here that the Kummer function of Eq. (2) not only represents the slope of the asymptotic tail but also the branching point of this tail from the central Gaussian-like function. Presence of multiple central peaks prohibit us to detect the proper branching point. Nevertheless, the proper value of B could be obtained by fitting all asymptotic tails together. The solid lines indicate the fits and the value of B obtained was 3.0 ± 0.4 Å^2.

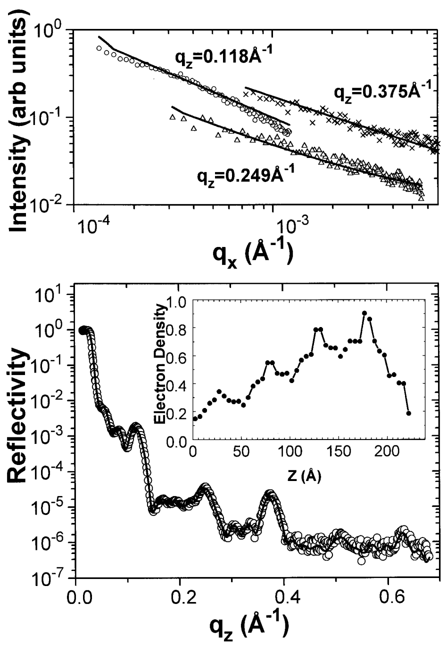

Fig. 3. Lower panel: (a) specular reflectivity and obtained electron density (electrons/Å^3) profile (in inset) for ferric stearate LB film (9 monolayers) are shown. The solid line is the calculated profile obtained from the model shown in inset. Upper panel: asymptotic tails of transverse diffuse scattering data measured at the first three Bragg peak positions (q_z values indicated) shown along with the fitted curves (solid lines). Refer to the text for details.

It is interesting to note that in case of the FeSt film the estimated value of the effective interfacial tension ($\gamma = \simeq 44$ mN m^{-1}) turns out to be quite close to the value of the surface tension of the monolayer from which the film was deposited. This indicates that no major structural rearrangement has taken place in this film after deposition, as is expected for a *preformed salt*. But for the CdA film the obtained value of effective interfacial tension ($\gamma \simeq 63$ mN m^{-1}) differs significantly from that of the acid monolayer used for LB deposition. This result indicates a possibility of structural rearrangements during deposition, due to the salt formation and the transfer process. However, we note that the effective interfacial tension of CdA film remains unchanged even after the CdS formation. We also observe that the molecular stacking of the LB film remains almost unchanged even after the chemical reaction, confining the formed CdS nanoparticles in the interfaces.

Acknowledgements

It is our pleasure to thank Prof. S.S. Major, Dr. A. Dhanabalan and Mr. N. Prashanth Kumar of the Department of Physics, Indian Institute of Technology, Mumbai, and Prof. J. Dutta of the Institute of Wetland Management and Ecological Design for their support in the sample preparation.

References

[1] M.K. Sanyal et al., Europhys. Lett. 36 (1996) 265; S. Banerjee et al., Phys. Rev. B 54 (1996) 16 377.

[2] S.K. Sinha et al., Phys. Rev. B 38 (1988) 2297.

[3] M.K. Sanyal et al., Mat. Res. Soc. Symp. Proc. 237 (1992) 393; S.K. Sinha et al., Physica B 198 (1994) 72.

[4] V. Holy, T. Baumbach, Phys. Rev. B 49 (1994) 10668.

[5] M.K. Sanyal et al., Phys. Rev. Lett. 66 (1991) 628.

[6] J. Zasadzinski et al., Sci. 263 (1994) 1726; G. Roberts (Ed.), Langmuir–Blodgett Films, Plenum, New York, 1990.

[7] I. Langmuir, Trans. Faraday Soc. 15 (1920) 62; K.B. Blodgett, J. Am. Chem. Soc. 57 (1935) 1007.

[8] V. Nitz et al., Phys. Rev. B 54 (1996) 5038; A Gibaud et al., Phys. Rev. Lett. 74 (1995) 3205.

[9] A. Malik et al., Phys. Rev. B 52 (1995) 11654.

[10] E.S. Smotkin et al., Chem. Phys. Lett. 152 (1988) 265; N.J. Geddes et al., J. Phys. Chem. 97 (1993) 13 767; P. Facci et al., Proc. Natl. Acad. Sci. USA 93 (1996) 10 556.

[11] A. Dhanabalan et al., Solid State Commun. 99 (1996) 859.

[12] A. Datta, M.K. Sanyal, A. Dhanabalan, S.S. Major, J. Phys. Chem. B101 (1997) 9280.

[13] A. Braslau et al., Phys. Rev. A 38 (1988) 2457; D. Schwartz et al., Phys. Rev. A 41 (1990) 5687; B.M. Ocko et al., Phys. Rev. Lett. 72 (1994) 242.

[14] J. Daillant, O. Belorgey, J. Chem. Phys. 97 (1992) 5824; 97 (1992) 5837.

[15] R. Holyst, Phys. Rev. A 44 (1991) 3692.

[16] I.M. Tidswell et al., Phys. Rev. Lett. 66 (1991) 2108.

[17] M. Sferraza et al., Phys. Rev. Lett. 78 (1997) 3693.

[18] M. Piecuch, L. Nevot, Mat. Sci. Forum 59/60 (1990) 93.

[19] M.K. Sanyal et al., J. Synchrotron Rad. 4 (1997) 185.

[20] J.K. Basu, M.K. Sanyal, Phys. Rev. Lett. 79 (1997) 4617.